1-1-2015

CW dual-frequency MOPA laser with frequency separation of 45 GHz

Miao Hu
University of Central Florida

Yaoyuan Zheng

Ju Cai

Guiju Zhang

Qiliang Li

See next page for additional authors

CW dual-frequency MOPA laser with frequency separation of 45 GHz

Miao Hu,[1,2,*] Yaoyuan Zheng,[1] Ju Cai,[3] Guiju Zhang,[4] Qiliang Li,[1] Xuefang Zhou,[1] Yizhen Wei,[1] and Yang Lu[1]

[1]*College of Communication Engineering, Hangzhou Dianzi University, Hangzhou, Zhejiang 310018, China*
[2]*CREOL, The College of Optics & Photonics, University of Central Florida, Orlando, Florida 32816, USA*
[3]*College of Communication Engineering, Chengdu University of Information Technology, Chengdu, Sichuan 610000, China*
[4]*Jiangsu Province Key Laboratory of Modern Optical Technology, Soochow University, Suzhou, Jiangsu 215006, China*
[*]*miao_hu@foxmail.com*

Abstract: A CW dual-frequency master oscillator power amplifier (MOPA) laser system with dozens of gigahertz (GHz) frequency separation is presented. The MOPA system consists of a monolithic microchip seed laser and a double-end pumped traveling wave power amplifier. The short length of seed laser cavity guarantees the seed signal with a large frequency separation (above 53 GHz) but low output power (below 247.8 mW). By adding a long and low-doped active medium laser amplifier stage, a significant increase in laser power and an improvement in beam quality are obtained. After fine temperature tuning of seed laser cavity for "spectra matching", a 2.40 W dual-frequency laser signal with 45 GHz frequency separation is achieved.

OCIS codes: (140.3480) Lasers, diode-pumped; (060.5625) Radio frequency photonics.

References and links

1. Y. Tan, S. Zhang, and Y. Zhang, "Laser feedback interferometry based on phase difference of orthogonally polarized lights in external birefringence cavity," Opt. Express **17**(16), 13939–13945 (2009).
2. W. Mao, S. Zhang, L. Cui, and Y. Tan, "Self-mixing interference effects with a folding feedback cavity in Zeeman-birefringence dual frequency laser," Opt. Express **14**(1), 182–189 (2006).
3. G. Baili, L. Morvan, M. Alouini, D. Dolfi, F. Bretenaker, I. Sagnes, and A. Garnache, "Experimental demonstration of a tunable dual-frequency semiconductor laser free of relaxation oscillations," Opt. Lett. **34**(21), 3421–3423 (2009).
4. G. Kervella, J. Maxin, M. Faugeron, P. Berger, H. Lanctuit, G. Pillet, L. Morvan, F. Dijk, and D. Dolfi, "Laser Sources for Microwave to Millimeter-wave Applications," Photon. Res. **2**(4), B70–B79 (2014).
5. A. Rolland, M. Brunel, G. Loas, L. Frein, M. Vallet, and M. Alouini, "Beat note stabilization of a 10-60 GHz dual-polarization microlaser through optical down conversion," Opt. Express **19**(5), 4399–4404 (2011).
6. G. Danion, C. Hamel, L. Frein, F. Bondu, G. Loas, and M. Alouini, "Dual frequency laser with two continuously and widely tunable frequencies for optical referencing of GHz to THz beatnotes," Opt. Express **22**(15), 17673–17678 (2014).
7. G. Pillet, L. Morvan, M. Brunel, F. Bretenaker, D. Dolfi, M. Valet, J. Huignard, and A. L. Floch, "Dual-Frequency Laser at 1.5 um for Optical Distribution and Generation of High-Purity Microwave Signals," J. Lightwave Technol. **26**(15), 2764–2773 (2008).
8. S. De, A. El Amili, G. H. Loas, S. Schwartz, G. Feugnet, J. Pocholle, F. Bretenaker, and M. Alouini, "Intensity Noise Reduction of Dual-Frequency Nd:YAG Lasers," in *International Conference on Fiber Optics and Photonics*, OSA Technical Digest (online) (Optical Society of America, 2012), paper T3B.2.
9. M. Brunel, F. Bretenaker, S. Blanc, V. Crozatier, J. Brisset, T. Merlet, and A. Poezevara, "High-spectral purity RF beat note generated by a two-frequency solid-state laser in a dual thermo optic and electrooptic phase-locked loop," IEEE Photon. Technol. Lett. **16**(3), 870–872 (2004).
10. A. McKay and J. M. Dawes, "Tunable terahertz signals using a helicoidally polarized ceramic microchip laser," IEEE Photon. Technol. Lett. **21**(7), 480–482 (2009).
11. Y. Qiao, S. Zheng, H. Chi, X. Jin, and X. Zhang, "Electro-optically tunable microwave source based on composite-cavity microchip laser," Opt. Express **20**(27), 29090–29095 (2012).
12. R. Cheng and S. Zhang, "Diode-pumped dual-frequency microchip Nd: YAG laser with tunable frequency difference," Appl. Phys. (Berl.) **42**(15), 155107 (2009).

#234260 - $15.00 USD Received 10 Feb 2015; revised 15 Mar 2015; accepted 2 Apr 2015; published 9 Apr 2015

13. J. Le Gouët, J. Xi, L. Morvan, M. Alouini, J. Bourderionnet, D. Dolfi, and J. P. Huignard, "Dual-frequency single-axis laser using a lead lanthanum zirconate tantalate (PLZT) birefringent etalon for millimeter wave generation: Beyond the standard limit of tunability," Opt. Lett. **32**(9), 1090–1092 (2007).
14. M. Brunel, A. Amon, and M. Vallet, "Dual-polarization microchip laser at 1.53 μm," Opt. Lett. **30**(18), 2418–2420 (2005).
15. M. Hu, R. An, H. Zhang, Q. Huang, and J. Ge, "Experimental investigation of a novel microchip laser producing synchronized dual-frequency laser pulse with an 85 GHz interval," Laser Phys. Lett. **10**(1), 015801 (2013).
16. P. Zhao, S. Ragam, Y. J. Ding, and I. B. Zotova, "Investigation of terahertz generation from passively Q-switched dual-frequency laser pulses," Opt. Lett. **36**(24), 4818–4820 (2011).
17. V. K. Bagdasarov, N. N. Denisov, A. A. Malyutin, and I. A. Chigaev, "Pulse synchronisation in passively Q-switched lasers emitting at 1.053 and 1.064 μm," Quantum Electron. **39**(10), 887–890 (2009).
18. H. P. H. Cheng, P. Tidemand-Lichtenberg, O. B. Jensen, P. E. Andersen, P. M. Petersen, and C. Pedersen, "All passive synchronized Q-switching of a quasi-three-level and a four-level Nd:YAG laser," Opt. Express **18**(23), 23987–23993 (2010).
19. X. Wang, T. Riesbeck, and H. J. Eichler, "Tunable single frequency microchip Nd: YAP MOPA laser operating at 1.08 μm," Laser Phys. **23**(4), 045804 (2013).
20. X. Yan, Q. Liu, X. Jiang, D. Wang, and M. Gong, "The combined guiding effect in MOPA lasers," Laser Phys. Lett. **10**(4), 045003 (2013).
21. Z. Xiang, D. Wang, S. Pan, Y. Dong, Z. Zhao, T. Li, J. Ge, C. Liu, and J. Chen, "Beam quality improvement by gain guiding effect in end-pumped Nd:YVO_4 laser amplifiers," Opt. Express **19**(21), 21060–21073 (2011).
22. Z. Ye, Z. Zhao, S. Pan, X. Zhang, C. Wang, Y. Qi, C. Liu, Z. Xiang, and J. Ge, "Beam profile evolution and beam quality changes inside a diode-end-pumped laser oscillator," IEEE J. Quantum Electron. **50**(2), 62–67 (2014).
23. Y. Qi, Z. Zhao, C. Liu, and Z. Xiang, "Beam quality management in multi-stage side-pumped Nd: YAG MOPA laser systems," IEEE J. Sel. Top. Quantum Electron. **21**(1), 1–6 (2015).
24. T. Yoshino and Y. Kobayashi, "Temperature Characteristics and Stabilization of Orthogonal Polarization Two-Frequency Nd^{3+}:YAG Microchip Lasers," Appl. Opt. **38**(15), 3266–3270 (1999).
25. N. P. Schmitt, P. Peuser, S. Heinemann, and A. Mehnert, "A model describing the single and multiple line spectra of tunable microcrystal lasers," Opt. Quantum Electron. **25**(8), 527–544 (1993).
26. W. Koechner, *Solid-State Laser Engineering* (Springer, 2006).
27. A. E. Siegman, *Lasers* (University Science Books, 1986).
28. Y. Huang, Z. Wei, K. Su, and Y. Chen, "Power scaling in a diode-end-pumped multisegmented Nd:YVO_4 laser with double-pass power amplification," IEEE J. Sel. Top. Quantum Electron. **21**(1), 1601006 (2015).
29. A. Agnesi, P. Dallocchio, F. Pirzio, and G. Reali, "Sub-nanosecond single-frequency 10-kHz diode-pumped MOPA laser," Appl. Phys. B **98**(4), 737–741 (2010).

1. Introduction

The field of microwave photonics has attracted growing interests worldwide in recent years, with applications such as metrology [1, 2], remote sensing [3], communication systems [4] as well as photonic radio frequency (RF) wave and terahertz (THz) wave generation [5, 6]. Among different architectures of photonic RF wave generation, the adoption of dual-frequency lasers is an interesting way, in which dual frequency signals oscillate in the same cavity for frequency beating. Dual-frequency microchip lasers based RF wave sources offer advantages in terms of low phase noise [7–9], frequency tunability [10–14] and direct modulation schemes [10]. Unfortunately, the output power of microchip laser is limited (mostly less than hundreds of milliwatts) due to the sufficiently short cavity (which means the gain medium length is also short). Since the heterodyning efficiency is squarely dependent on the laser intensity, the output power scales of microchip laser brings a limitation to its applicability of photonic RF source.

For pulsed photonic RF and THz source, Q-switched dual-frequency lasers are good solution for heterodyning efficiency enhancement because of their high peak power output. Comparing to actively Q-switched lasers, passively Q-switched lasers have a great advantage of compactness, which is very needed for microchip laser operation. By employing Nd^{3+}:Cr^{4+}:YAG co-doped laser crystals or Cr^{4+}:YAG crystals in laser cavity as Q switchers, passively Q-switched dual-frequency pulsed lasers were achieved in ultra-compact structures with frequency separation from gigahertz (GHz) to THz [15–18]. However, the pulses generated by these lasers suffer from large timing jitters. Some efforts, such as by precise temperature controllers [15] and specific cavities [16–18] are exploited to reduce the timing jitters between the dual-frequency pulses train, synchronization have yielded a timing jitter as low as tens of nanoseconds.

#234260 - $15.00 USD Received 10 Feb 2015; revised 15 Mar 2015; accepted 2 Apr 2015; published 9 Apr 2015

An approach for achieving power scalability of dual-frequency laser is referred to as the master oscillator power amplifier (MOPA) configuration, in which a master oscillator produces a seed laser with specified time and frequency domain feathers and an optical amplifier is used for power amplification while preserving the properties of the seed laser [19]. The MOPA systems present an effective way to produce a high average power CW dual-frequency laser, which is very useful for CW photonic RF and THz wave generation. Nevertheless, the thermally induced wavefront distortions in the gain media of amplifiers sometimes degrade the beam quality; the M^2 factors of the final amplified laser beams are often larger than that of the master oscillators. By using relay optics, Liu *et al.* presented solutions [20–23], in which laser beams are coupled in the amplifiers by free space propagation. The gain media in amplifiers act as soft apertures, which can reshape the beam intensity distributions by amplifying the central part of the beam. While the amplifiers are properly positioned, the beam quality improvement can be realized, as well as acceptable extraction efficiency.

Here, we propose a high-power dual-frequency laser setup based on a Nd:YVO_4 microchip laser and a double-end pumped amplifier. The spectral narrowing of the dual mode difference frequency caused by the amplifier gain width is analyzed. The paper is organized as follows. In chapter 2, the theoretical modeling is presented for dual-frequency modes operation in a MOPA system. In chapter 3, an experimental setup of dual-frequency MOPA system is built up, the output power and optical spectra are then investigated. Conclusions are drawn in the last chapter.

2. Theoretical modeling

Here, a monolithic dual modes microchip laser was adopted as the seed laser. In such a laser, the frequency separation is inherently more stable than that in a separated laser, and the free-running state induced frequency instability can be improved by means of feedback control [24]. Schmidt *et al.* gave a detailed theoretical model for describing the spectral lines of microchip lasers [25]. In his theory, the maximum number of modes m within the gain profile (Lorenz distribution) is given by:

$$m = 2\Delta v_0 nL / c \tag{1}$$

where Δv_0 is the gain bandwidth of laser, c is the velocity of light in vacuum, n is the refractive index and L is the geometrical length of the laser cavity. The dual modes resonating in a microchip laser is guaranteed by the precise length of laser cavity.

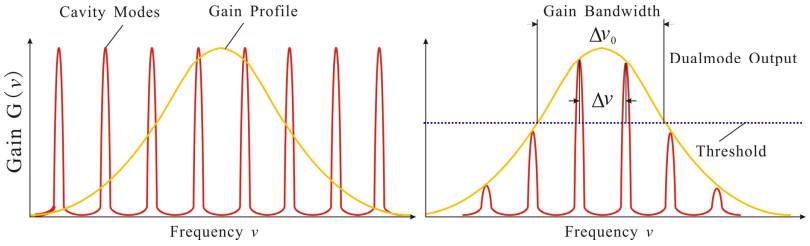

Fig. 1. The spectrum of dual modes operates in a monolithic microchip laser. The longitudinal mode spacing $\Delta v = c/2nL$ is larger than the half and less than the entire gain bandwidth ($\Delta v_0 > \Delta v > \Delta v_0/2$). Only dual-longitudinal modes (red lines) can exceed the threshold and start to oscillate.

In Fig. 1, the spectral scheme of dual-mode oscillation in a microchip laser cavity is depicted. According to Fig. 1, the longitudinal mode spacing Δv is kept larger than the half and less than the entire laser gain bandwidth ($\Delta v_0 > \Delta v > \Delta v_0/2$). The gain bandwidth of laser is related to the fluorescence spectrum of the laser medium, the pump level and the laser cavity loss. By cutting the microchip laser with a precise length ($c/\Delta v_0 n > L > c/2\Delta v_0 n$), maintaining the

#234260 - $15.00 USD Received 10 Feb 2015; revised 15 Mar 2015; accepted 2 Apr 2015; published 9 Apr 2015

pump in an appropriate level and using an output mirror with proper reflectivity, dual-longitudinal modes oscillation was achieved.

In order to make sure the dual modes of the seed laser have approximately equal amplification efficiencies, the dual-mode wavelengths have to be located quasi-symmetrically with respect to the gain profile center of the amplifier, which is named "spectra matching". Since the gain profile center of a travelling wave amplifier is basically only related to the gain profile of laser medium, the "spectra matching" can be realized by wavelength tuning of the seed laser. By utilizing the natural characteristic of the wavelength shifting induced by the microchip laser cavity temperature variation [19], the seed laser wavelengths tuning can be achieved by a simple temperature controller. Generally, the thermally induced wavelength change of a microchip laser can be revealed by the thermal expansion coefficient α_e and temperature variation of the refractive index dn/dT of the laser material [26]. For Nd:YVO_4 microchip lasers, the wavelength change versus the temperature of laser cavity can be expressed as follows:

$$d\lambda / dT = \lambda[\alpha_e + (1/n) * dn / dT] \tag{2}$$

The related specifications of a-cut Nd:YVO_4 crystal are α_e = 11.37 × 10^{-6} /K, n = 2.16 and dn/dT = 2.9 × 10^{-6} /K; the $d\lambda/dT$ was calculated to be 13.47 × 10^{-3} nm/K. Further, during the amplification process, the finite gain bandwidth of the amplifier will make the laser spectra undergo significant evolutions with respect to the input spectra such as narrowing of the frequency difference of the two modes. Here, the bandwidth of the amplifier δv_{SH} is related to the total gain $g^0(v_0)L$ as well as the atomic linewidth Δv_H of the laser medium, g^0 is the gain constant, L is the gain length. When total gain $g^0(v_0)L >> 1$, the δv_{SH} can be expressed as [27]:

$$\delta v_{SH} \approx \Delta v_H \sqrt{\ln 2 / g^0(v_0) L} \tag{3}$$

3. Experimental analyses

The experimental dual-frequency MOPA system setup is shown in Fig. 2. The system consists of two parts, a microchip laser and a power amplifier. The monolithic microchip laser resonator was formed by a pair of plane parallel crystal surfaces. The input surface film have a reflectivity R>99.8% at 1064 nm and a transmittance T>96.0% at 808 nm. The output surface film have a reflectivity R = 80% at 1064 nm and a reflectivity R>96.0% at 808 nm. The fiber coupled laser diode (LD) offered a maximum 5.0 W pump power with central wavelength at 808 nm. The output fibers have a core diameter of 400 μm and a numerical aperture (NA) of 0.22. The pump beam was focused into the Nd:YVO_4 microchip crystal by using a GRIN Lens (Ø1.8 mm, 0.29 Pitch, Uncoated). The Nd doping concentration of laser crystal is 1.0% and the dimension is 3 mm × 3 mm × 1.2 mm (Castech inc.), a-cut. The absorption coefficient at pump wavelength is 31.3cm^{-1}@808nm. For better thermal contact and reducing the deleterious thermal effects, the Nd:YVO_4 crystal was wrapped with a piece of 0.1 mm thick indium foil and mounted in a semiconductor cooled copper sink. The generated dual-frequency seed laser was reflected into the amplifier by mirrors and dichroic mirrors (DM). Kepler telescope was used to guarantee good mode overlap between the seed laser beam and the gain area of amplifier.

A double-end LD pumped "U" type Nd:YVO_4 travelling wave amplifier configuration was employed. The Nd doping concentration of gain medium crystal is 0.3%, and the dimension is 3 mm × 3 mm × 12 mm (Castech inc.). Such a long and low doped crystal not only offers large gain levels but also keeps the beam quality stable by uniforming the absorption of pumping power in length and moderating the thermal effects in amplification process. The Nd:YVO_4 crystal was also wrapped with a piece of 0.1 mm thick indium foil and mounted in a semiconductor cooled copper sink. Two high-brightness fibers coupled LDs, each with a maximum output power of 50 W, were used as the pump sources. The output fibers have a core diameter of 400 μm and a NA of 0.22. Each fiber end was imaged to the

#234260 - $15.00 USD Received 10 Feb 2015; revised 15 Mar 2015; accepted 2 Apr 2015; published 9 Apr 2015

closer end face of Nd:YVO_4 laser crystal with a pump diameter of 800 μm through a pair of positive spherical lenses. Two DMs, with a reflectivity R>99.8% at 1064 nm and a transmittance T>90.0% at 808 nm for 45° beam incidence angle, formed a "U"-type amplification structure. The seed laser beam was reflected into the amplifier by DM_1 and the amplified laser beam was reflected out by DM_2.

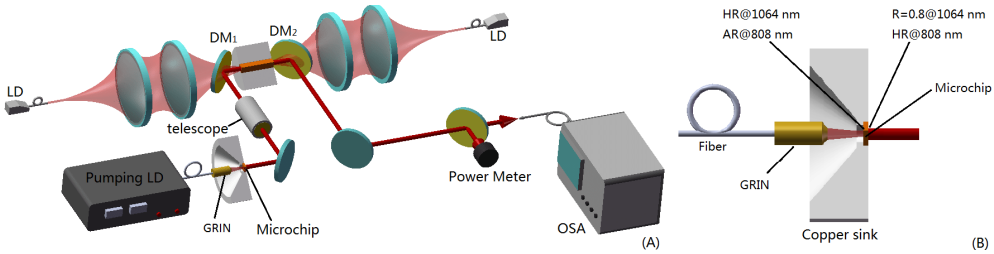

Fig. 2. Experimental setup of the "U" type dual-frequency MOPA laser system. GRIN: GRIN lens. OM: output mirror. DM: dichroic mirrors. OSA: optical spectrum analyzer.

The π polarized output power of seed laser (P_{SL}) was investigated experimentally using a power meter (PM10X, Coherent Inc.). The P_{SL} versus pump power of seed laser (P_{SLD}) and pump current of seed laser (C_{SLD}) is shown in Fig. 3. With the temperature of copper sink uncontrolled, the threshold of the seed laser was measured as about 1.0 W (the corresponding LD current was 11.0 A). As C_{SLD} went up gradually from 12.1 A to 14.5 A, the P_{SLD} grew up from 1.43 W to 2.23 W, while P_{SL} presented a growth from 68.5 mW to 247.8 mW. The optical efficiency was fitted as a linear function with a slope of 24.34%. When P_{SLD} exceeded 2.40 W, the thermal induced stress and deformation would lead fragment of the front film of the microchip laser.

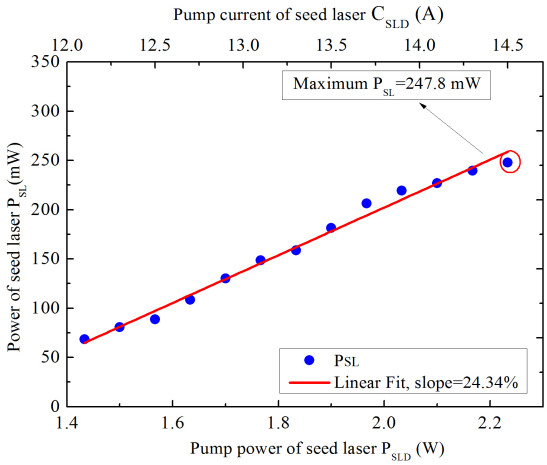

Fig. 3. The power of seed laser (P_{SL}) vs. pump power of seed laser (P_{SLD}) and pump current of seed laser (C_{SLD}). The optical efficiency was fitted as a linear function with a slope of 24.34%.

The deposited heat raises the temperature of the microchip laser with the increasing of P_{SLD}. Since the seed laser wavelengths positively correlated to the temperature of the laser cavity, the wavelengths red shifted along with the increasing of P_{SLD}. The optical spectra of seed laser (S_{SL}s) with different P_{SLD} were obtained by an OSA (AQ6370B, Yokogawa Inc.) with a resolution of 0.02 nm. The "mode hopping" was observed in seed laser due to the short cavity length, and made the wavelengths shift periodically within a certain range, shown in Fig. 4. The seed laser operated as single longitudinal mode when P_{SLD} was below 1.70 W. As P_{SLD} increased from 1.56 W to 1.63 W, the arithmetic central wavelength of seed laser (CW_{SL}) shifted from 1064.24 nm to 1064.30 nm. A higher P_{SLD} was required for dual-frequency modes operation. When P_{SLD} increased from 1.70 W to 1.90 W, the CW_{SL} shifted

#234260 - $15.00 USD Received 10 Feb 2015; revised 15 Mar 2015; accepted 2 Apr 2015; published 9 Apr 2015

from 1064.11 nm (Pk_L: 1064.01 nm, right peak Pk_R: 1064.21 nm) to 1064.35 nm (Pk_L: 1064.25 nm,Pk_R: 1064.45 nm); when the P_{SLD} increased from 1.96 W to 2.16 W, the CW_{SL} shifted from 1064.10 nm (Pk_L: 1064.00 nm, Pk_R: 1064.20 nm) to 1064.31 nm (Pk_R: 1064.21 nm,Pk_R: 1064.41nm). Since the cavity optical length L_R (L_R=nL) of seed laser was designed to ensure the longitudinal mode spacing is larger than the half and less than the whole of gain bandwidth, only single or dual modes resonated in the cavity within the whole P_{SLD} range.

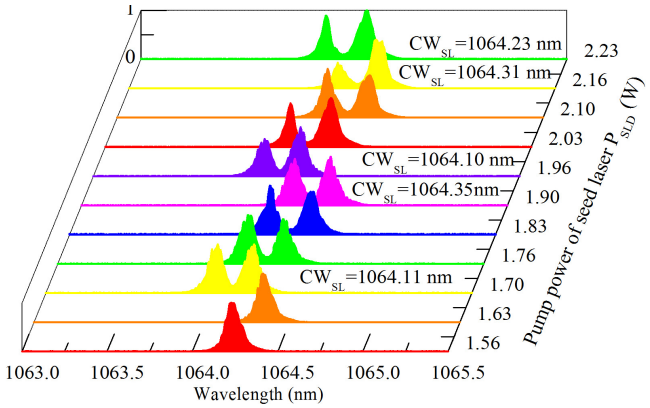

Fig. 4. The spectra of seed laser (S_{SL}s) vs. P_{SLD}. When P_{SLD} is below 1.70 W, the seed laser remained as single mode output. When P_{SLD} increased from 1.70 W to 2.23 W, dual-mode signals appeared and the wavelengths red-shifted. The "mode hopping" made the wavelengths shift periodically within a certain range.

The seed laser beam went into the double-end pumped travelling wave amplifier through a Kepler telescope and a distance of free space for better mode overlap. The pump current of the amplifier C_{ALD} was kept at 40.0 A for both ends, and the amplifier crystal temperature was keep at 20.0°C. 0.36 W power of amplified laser (P_{AL}) was achieved with P_{SLD} of 1.23 W. As P_{SLD} went up to 2.23 W, the P_{AL} approached 2.38 W. Comparing the P_{AL} with the P_{SL} in different P_{SLD}, the corresponding amplification factor (A.F.) was calculated. The diagram of P_{AL} and A.F. vs. P_{SLD} was shown in Fig. 5.

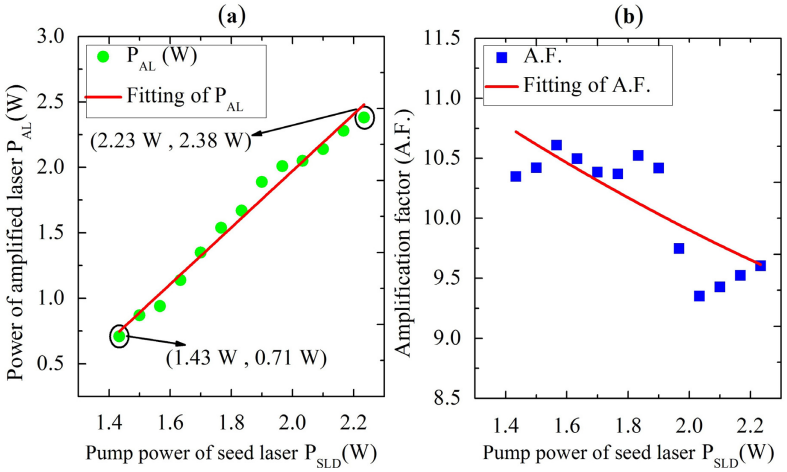

Fig. 5. The pump current of amplifier (C_{ALD}) in both ends was kept at 40 A; and the P_{SLD} increased from 1.43 W to 2.23 W. (**a**) power of amplified laser (P_{AL}) vs. P_{SLD} (green solid circle dots). The P_{AL} ranges from 0.71 W to 2.38 W. (**b**) The amplification factor (A.F.) vs. the P_{SLD} (blue solid rectangles). The A.F. ranges from 9.35 to 10.65.

#234260 - $15.00 USD Received 10 Feb 2015; revised 15 Mar 2015; accepted 2 Apr 2015; published 9 Apr 2015

In Fig. 5(b), due to the "spectra matching", the A.F. curve fluctuated with the increase of the P_{SLD}. The small signal measurements revealed the gain bandwidth of amplifier ranged from 1063.9 nm to 1064.6 nm, and the center was at 1064.25 nm, approximately. The seed lasers whose wavelengths stayed closer to the gain profile center yielded higher amplification efficiency; and those away from the gain center yielded lower amplification efficiency. While P_{SLD} were 1.56 W, 1.83 W, 2.23 W, the CW_{SL} were measured as 1064.24 nm, 1064.27 nm (Pk_L: 1064.16 nm, Pk_R: 1064.38 nm), 1064.23 nm (Pk_L: 1064.12 nm, Pk_R: 1064.33 nm), the A.F. reached 10.65, 10.55, 9.65 maximally, respectively. Meanwhile, because of the gain saturation effect of the amplifier, the amplification efficiency decreases on the whole with P_{SLD} increases from 1.43 W to 2.23 W. In order to characterize the gain saturation effect of the amplifier, the A.F. = G_{AL} was fitted by using Frantz-Nodvik model [28, 29]:

$$G_{AL} = P_{sat}/P_{SL} \ln\left\{1+G_0\left[\exp\left(P_{SL}/P_{sat}\right)\right]\right\} \quad (4)$$

Here, the saturation parameter and small-signal gain are characterized by P_{sat} = 7 W and G_0 = 11.2, respectively. Comprehensively, the "spectra matching" together with the gain saturation effect made the A.F. increase gently and decrease more severely with the increase of the P_{SLD}.

The fine "spectra matching" was realized by careful temperature tuning of the microchip laser cavity. The P_{SLD} was kept at 2.23 W for maximum P_{SL} output. Gain profiles of the amplifier are shown by black dash lines in Fig. 6. The S_{SL}s are shown in Fig. 6(a)-6(c) with the laser cavity temperatures of 45.1°C, 53.3°C and 61.3°C in blue solid lines. The spectra of amplified laser (S_{AL}s) are shown in red lines. The CW_{SL} were measured as 1064.18 nm, 1064.23 nm and 1064.28 nm in Fig. 6(a)-6(c), the shift of the CW_{SL} vs. temperature was fitted as a linear function with a rate of 6 pm/°C, relatively low comparing with the result by Eq. (3). The CW_{AL} was measured as 1064.20 nm, 1064.24 nm, and 1064.26 nm. In Fig. 6, when the temperature was 45.1°C, the CW_{SL} was on the short-wavelength side of the gain maximum (about 1064.25 nm), the short-wavelength spectral component of S_{AL} displayed a significant red shift and the long-wavelength spectral component displayed a slight blue shift. As a result, the wavelength difference became smaller comparing to S_{SL}; and the P_{AL} was measured as 2.33 W. As the temperature was 61.3°C, the CW_{SL} was located on the long-wavelength side of the gain maximum, the long-wavelength spectral component of S_{AL} displayed a significant blue shift and the short-wavelength spectral component displayed a slight red shift. The wavelength difference also became smaller comparing to S_{SL}; and the P_{AL} was measured as 2.37 W. When the temperature was 53.3°C, the CW_{SL} was closed to the gain maximum and the dual modes shared nearly equal gain. The S_{AL} showed red shift in short-wavelength spectral component and blue shift in long-wavelength spectral component, nearly equally. The wavelength difference became smaller as well, and the P_{AL} reached the maximum, 2.40 W. A higher output power can be realized by using a next-stage amplifier.

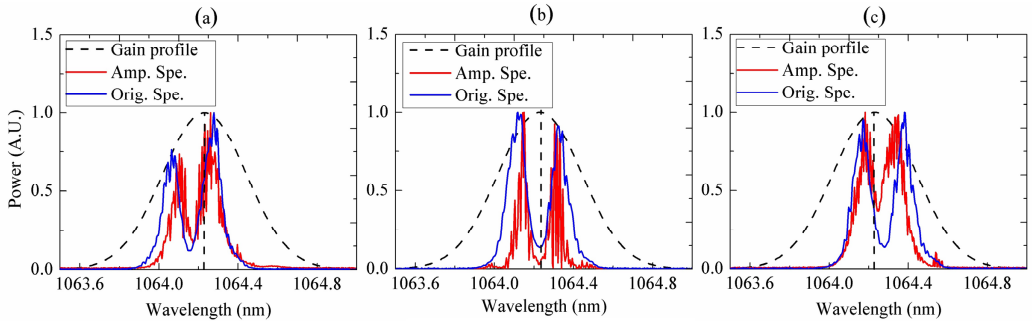

Fig. 6. The spectra of dual-frequency laser with 2.23 W P_{SLD} and different cavity temperatures. Gain profiles are in black dash lines. Spectra of the seed laser (S_{SL}s) are in blue lines. Spectra of amplified laser (S_{AL}s) are in red lines. (**a**) Temperature at 45.1°C. (**b**) Temperature at 53.3°C. (**c**) Temperature at 61.3°C.

#234260 - $15.00 USD Received 10 Feb 2015; revised 15 Mar 2015; accepted 2 Apr 2015; published 9 Apr 2015

The wavelength differences of seed lasers measured in Fig. 6(a)-6(c) were 0.21 nm, 0.21 nm and 0.20 nm, corresponding to 55.64 GHz, 55.63 GHz, and 53.01 GHz in frequency separation. After amplification, the wavelength differences of amplified lasers were measured of 0.16 nm, 0.17 nm and 0.16 nm, corresponding to 42.38 GHz, 45.03 GHz, and 42.37 GHz. The frequency separations of amplified laser signal became 22%~26% narrower than that of seed laser, which is the result of the finite gain bandwidth of the amplifier.

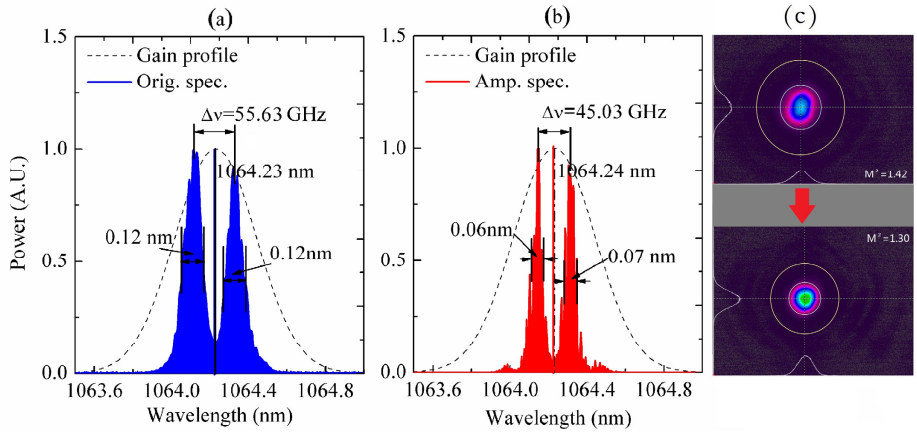

Fig. 7. Spectra of dual-frequency laser with P_{SLD} at 2.23 W and temperature at 53.3°C. The gain profiles are represented in black lines. (**a**) S_{SL} is of blue area. (**b**) S_{AL} is of red area. (**c**) The beam quality comparison between seed laser and amplified laser.

In Fig. 7(a) and 7(b), dual-frequency laser spectra with P_{SLD} at 2.23 W, P_{AL} at 2.40 W and temperature at 53.3°C are shown in details. The dual wavelengths of seed laser were measured as 1064.12 nm (the linewidth was 0.12 nm, corresponding to 31.79 GHz) and 1064.33 nm (the linewidth was 0.12 nm, corresponding to 31.78 GHz). The dual wavelengths of amplified laser were measured as 1064.15 nm (the linewidth was 0.06 nm, corresponding to 15.89 GHz) and 1064.32 nm (the linewidth was 0.07 nm, corresponding to 18.53 GHz). The black dash lines represent the gain profiles of amplifier. According to Eq. (3), the linewidth narrowing of each wavelength is the result of the finite gain bandwidth of the amplifier. The waveforms fringe were found in the S_{AL} but not in the S_{SL} meant the existence of noise in amplification process. By means of a beam profiler (BeamMaster, Coherent Inc.), the M^2 factor of seed laser beam and amplified laser beam were measured as 1.42 and 1.30, respectively, shown in Fig. 7(c). The beam quality improvement is due to the gain guiding effect. In the experimental setup, the beam from the seed laser was firstly expanded by a telescope, and then propagated a free space to the incident plane of the amplifier. The beam intensity distribution slightly changed as it propagates. The amplifier was positioned in the plane where the beam had a nearly Gaussian distribution in the center and a halo light in the margin. The gain guiding effect in the amplifier can thus improve the beam quality by amplifying the central part of the beam. The enhancement of beam quality agreed with the linewidth narrowing of amplified laser. The narrow linewidth and the good beam quality of the high-power amplified lasers made it easier to generate millimeter-wave signals with higher purity.

4. Conclusion

A dual-frequency MOPA system was demonstrated experimentally. The system consisted of a dual-frequency monolithic Nd:YVO_4 microchip master seed laser and a Nd:YVO_4 power amplifier. The central wavelength of the seed laser was tuned by changing the temperature to approach the gain maximum ("spectra matching") in amplification. Through the MOPA system, a dual-frequency laser with 2.40 W output power and 45.03 GHz frequency separation with was achieved.

#234260 - $15.00 USD Received 10 Feb 2015; revised 15 Mar 2015; accepted 2 Apr 2015; published 9 Apr 2015

Acknowledgments

This work was funded by Nature Science Funds of Zhejiang Province (Grant Number: LQ13F010012), and supported by Zhejiang Provincial Key Lab of Data Storage and Transmission Technology, Hangzhou Dianzi University

#234260 - $15.00 USD Received 10 Feb 2015; revised 15 Mar 2015; accepted 2 Apr 2015; published 9 Apr 2015